

# Oriented, Single Domain Fe Nanoparticle Layers in Single Crystal Yttria-Stabilized Zirconia

Korey D. Sorge, James R. Thompson, Thomas C. Schulthess, Frank A. Modine, Tony E. Haynes, Shin-ichi Honda, Alkiviathes Meldrum, John D. Budai, C. W. White, and Lynn A. Boatner

**Abstract**—To create an ensemble of oriented, single crystal particles of iron, Fe ions were implanted into the near-surface region of single crystal yttria-stabilized zirconia (YSZ). With thermal processing, the implanted species precipitated to form faceted, predominantly single-domain ferromagnetic nanoparticles. The YSZ substrate isolates, protects, and crystallographically textures the nanoparticles, creating a magnetically anisotropic layer. Experimental studies of the magnetization  $M(H, T)$  at various orientations of the applied field  $H$  show a major distinction only between  $H \parallel \hat{n}$  (hard direction) and  $H \perp \hat{n}$  (easy direction) where  $\hat{n}$  is the surface normal; there is little angular variation within the plane. This feature and the behavior of the orientationally dependent coercive field  $H_c$  and magnetic remanence  $M_r$  are attributed to magnetostatic interactions between the particles. Non-interacting single-domain particles should show a Stoner–Wohlfarth-like behavior that is poorly approximated in this far-from-close-packed system.

**Index Terms**—Anisotropy, Fe nanoparticles, magnetostatic interactions, textured materials.

## I. INTRODUCTION

MINIATURIZATION interest in industry (with information storage being the most publicized) requires a new look at the properties of iron at the nanoscale. While magnetostatic properties of isolated single crystals small enough to be single domain are reasonably well understood [1]–[3], it is still unclear regarding how interparticle interactions can influence magnetic properties in an ensemble of Fe nanoparticles. For example, most experiments deal with particles that have an isotropic distribution of anisotropy axes. This single particle angular disorder mimics the frustration inherent in random interparticle dipolar interactions and provides qualitatively similar features, e.g., rounded  $M(H)$  curves. Thus, interactions are frequently neglected in the discussion of quasistatic magnetization curves [4] in dilute systems. However, for Fe particles in  $\text{SiO}_2$  [5], interactions have to be accounted for when the saturation magnetization is studied as a function of temperature. To clarify the issue of magnetostatic interactions, it is desirable to study an assembly of *crystallographically oriented* nanoparticles.

This is the subject of the present work, where a system of oriented single-domain, single-crystal Fe nanoparticles was

prepared in a buried, rather dilute, roughly 2D array. It provides a well-characterized system for examining how particle effective anisotropy competes with array shape anisotropy (related to interactions) in determining the magnetostatic characteristics.

## II. SAMPLE FABRICATION AND CHARACTERISTICS

Nanoparticles of  $\alpha$ -Fe have been formed in the near-surface region of single-crystal yttria-stabilized zirconia ( $\text{Y}_{0.2}\text{Zr}_{0.8}\text{O}_{1.9}$  or YSZ) by ion implantation followed by thermal processing. Singly-ionized  $^{56}\text{Fe}^+$  with an energy of 140 keV was implanted to a fluence of  $8 \times 10^{16}$  atoms/cm<sup>2</sup> providing a total Fe content of  $1.7 \times 10^{16}$  atoms, as measured by implant dose and RBS. Most of the implanted iron was present initially as isolated Fe in the YSZ with a Gaussian profile centered at a depth of  $\sim 45$  nm, according to TRIM calculations [6]. The Fe precipitated as single-crystal metal particles when the samples were annealed at high temperatures in a reducing atmosphere; a 1 h anneal in Ar + 4%  $H_2$  at 1000 °C with a slow cool, followed by a 2 h anneal in Ar + 4%  $H_2$  at 1100 °C that was quenched [7]. The thickness of the Fe array is  $\approx 80$  nm with a Gaussian profile that narrowed slightly with the annealing process and particle size is  $\lesssim 25$  nm, with a log-normal distribution. Particles of this size are expected to be nearly all single domain [3]. Furthermore, inspection of the TEM in Fig. 1 shows that the particles are well separated with a volume fraction of about 10%, well below the percolation limit.

The host matrix orients the newly-formed nanocrystals along distinct crystallographic directions, as illustrated in Fig. 2. Both the  $\alpha$ -Fe and YSZ are cubic, but the alignment is not cube-on-cube. Preferred orientation can be found by aligning all 3 cube axes of Fe with YSZ, and then rotating the Fe by 45° around a single  $\langle 100 \rangle$  [8]. In the present work, a substrate was selected with  $[110]$  along the normal of the surface, as illustrated.

## III. MAGNETIC MEASUREMENTS

Magnetic measurements were conducted in a superconducting quantum-interference device (SQUID) magnetometer at temperatures of 5–400K and in applied fields of up to 10 kOe. Because of the 3D texturing of the nanoparticles, it is possible to apply the field in several distinct crystallographic directions and to analyze the magnetic anisotropy of the system. Studies of magnetization  $M(H, T)$ , where  $H$  is the applied field and  $T$  is the temperature, provide detailed information about the system. In all cases, the background moment of YSZ (measured separately) was subtracted.

Manuscript received October 13, 2000.

This work was supported by the Laboratory Directed Research and Development Program of Oak Ridge National Laboratory (ORNL), managed by UT-Battelle, LLC for the U.S. Department of Energy under Contract DE-AC05-00OR22725.

The authors are with the Solid State Division, Oak Ridge National Laboratory, Oak Ridge, TN 37831-6061.

Publisher Item Identifier S 0018-9464(01)06519-0.

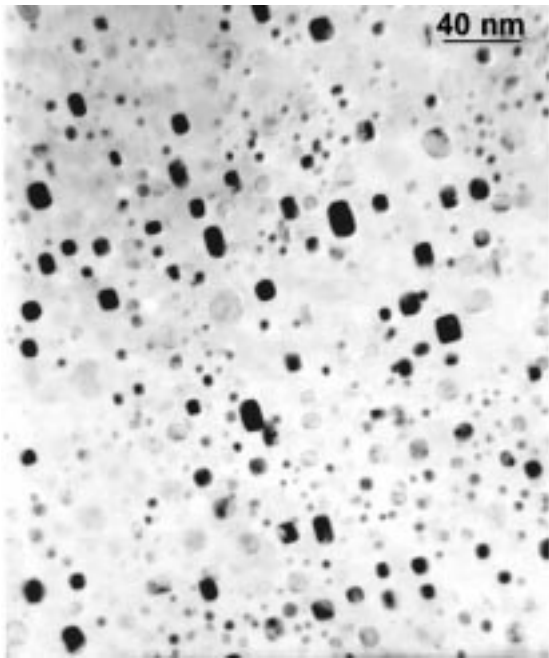


Fig. 1. TEM image of iron nanoparticles in the host substrate. Particles are  $\approx 25$  nm and volume fraction is  $\sim 10\%$ .

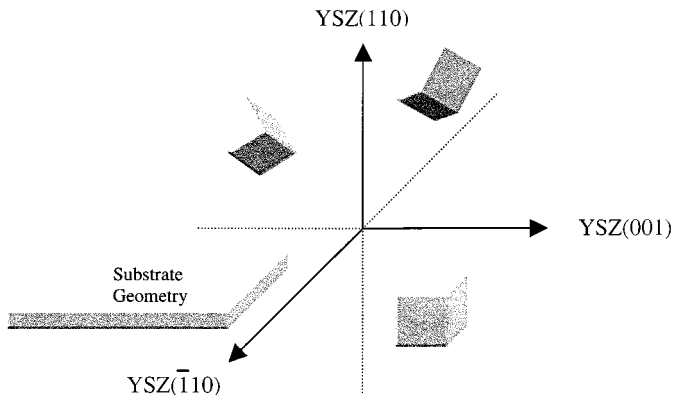


Fig. 2. Primary orientations of  $\alpha$ -Fe nanoparticles in YSZ [110], roughly equally populated.

Typical curves of magnetization as a function of applied field,  $M(H)$ , are given in Fig. 3. The saturation magnetization,  $M_{\text{sat}}$ , of the system at  $T = 5$  K is  $\sim 2.1 \mu_B/\text{atom}$ , compared to bulk  $\alpha$ -Fe with  $2.2 \mu_B/\text{atom}$  [2], a 6% difference that is within experimental error.

Several things can be noted in Fig. 3 when one considers the differences of the magnetization curve for different directions of the applied field. Most noticeably, the curve taken with the applied field perpendicular to the surface has the lowest remanence and the highest saturation field. This indicates that the anisotropy of the entire ensemble dominates. Furthermore, the coercivity appears to be insensitive to the direction of the applied field. With the field applied parallel to the layer, one expects a uniaxial anisotropy, since the (110) plane has only two-fold symmetry (see Fig. 2). Experimentally, the  $M(H)$  data exhibit only small differences in the remanence, a second order effect. Finally, the saturation field is always several times larger than the coercive field.

Let us now consider the variation of coercive field  $H_c$  and remanent magnetization  $M_r$ , with temperature. Fig. 4 shows that

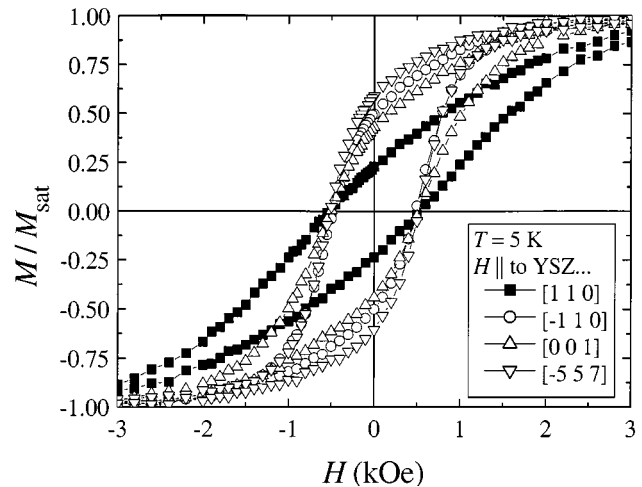


Fig. 3.  $M(H)$  curves for an array of Fe nanoparticles with differing orientations of applied field. The closed symbol signifies field applied along the array normal and the open symbols denote field applied along the surface.

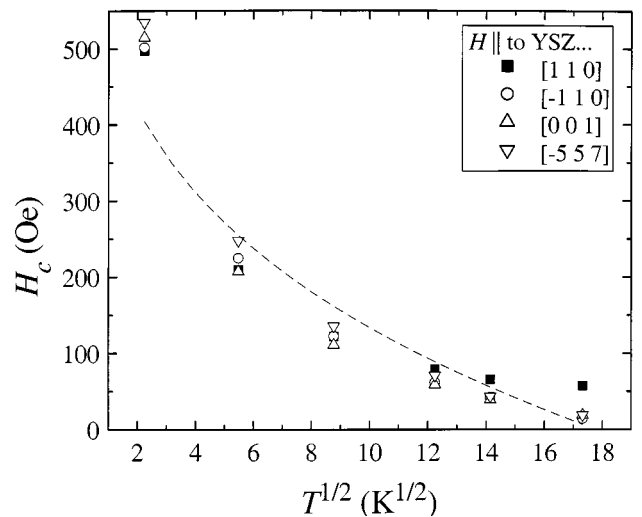


Fig. 4. The coercive field as a function of temperature, but not with the expected  $\sqrt{T}$  dependence. An empirical curve where  $n = 1/8$  and zero-temperature  $H_c = 1000$  Oe is shown.

$H_c$  changes little with differing applied field orientations, for all temperatures.  $H_c$  is suppressed with rising temperature when thermal activation excites the system over energy barriers. Fine, noninteracting particles with uniform size are predicted to have a temperature dependence of the form

$$\frac{H_c(T)}{H_c(0)} = 1 - \left( \frac{T}{T_B} \right)^n, \quad (1)$$

where  $T_B$  is the *blocking temperature* and  $n = 1/2$  for uniaxial anisotropy or  $2/3$  for cubic anisotropy [9]. The data shown in Fig. 4 deviate strongly from the  $\sqrt{T}$  or  $T^{2/3}$  dependence, which indicates that the assumption of independent, thermally-activated particles is not appropriate. To illustrate this point, we have used representative values for zero-temperature coercive field and the blocking temperature and show that the power-law dependence does not seem representative of the data.

The remanent magnetization  $M_r$  changes with differing applied field orientation. At low temperature, with  $H$  along the normal of the 2D array, we have  $M_r/M_{\text{sat}} \approx 0.25$  and with  $H$

along the surface of the array  $M_r/M_{\text{sat}} \approx 0.5$ . The in-plane orientational dependence of  $M_r/M_{\text{sat}}$ , which we attribute to magnetocrystalline anisotropy of the particles, is suppressed with increasing temperature, while the difference between in-plane and out-of-plane measurements persists to higher temperatures.

#### IV. DISCUSSION

Since the volume fraction of the magnetic particles in the present sample is small compared to the situation in typical granular films, one is tempted to neglect the interparticle interactions. However, let us consider the magnetic energy scales that are involved in our material. Since the particles are small enough to be in a single domain state with their magnetization rotating coherently during reversal, the three contributions to the energy of the particle assembly are 1) the Zeeman energy which couples the system to the applied field; 2) the effective anisotropy energy of the particles which includes the contributions of magnetocrystalline, shape, and surface anisotropy as well as possible magnetostrictive effects (since our particles are embedded in YSZ); and 3) the interparticle interaction energy that consists only of magnetostatic interactions, since there is no direct exchange between the isolated particles. Of these three energy terms, the latter two have to be compared to understand the magnetic properties of the system. A rough estimate for the ratio between the interparticle interaction and the effective anisotropy is given by  $\alpha \equiv 4\pi M_{\text{sat}}^2 f / 2K_{\text{eff}}$ , where as we have seen earlier, the volume fraction,  $f$ , is of the order of 10% and saturation magnetization is comparable to that of bulk Fe, i.e.,  $M_{\text{sat}} \approx 1700$  G. The effective anisotropy parameter,  $K_{\text{eff}}$ , is usually difficult to estimate, since in small particles, the unknown surface and shape anisotropies can be much more important than the magnetocrystalline anisotropy (rather small in Fe). For example, Chien [5] concluded that for Fe particles in  $\text{SiO}_2$  the effective anisotropy is several orders of magnitude larger than the bulk magnetocrystalline anisotropy. In the present case, however, we know that the particles are near-perfect cubes [7], [8], for which the surface anisotropy cancels by symmetry. The shape anisotropy of cubic particles has the same symmetry as the intrinsic magnetocrystalline anisotropy. It is therefore reasonable to assume that  $K_{\text{eff}} \approx 5 \times 10^5$  erg/cm<sup>3</sup>. This leaves us with  $\alpha \approx 3.8$ , meaning that interparticle interactions play a major role in this uniquely well-defined system of nanoparticles.

The magnetization curves of Fig. 3 reinforce this conclusion. The hard axis perpendicular to the particle array, the saturation field being much higher than the coercivity, and the simple observation that the asymmetric shape of the particle assembly as a whole is significant, all indicate that the particles are not independent. Additionally, it is not surprising that the power-law temperature dependence for  $H_c(T)$ , Eq. (1), fails when interactions are important. These figures, in conjunction with Fig. 5 showing the more persistent effects of array shape over individual particle anisotropy, all imply directly that the contribution of the effective anisotropy of the particles to the total energy is smaller than the interparticle interaction energy.

Finally, we note that the result of the present discussion, namely that interparticle interactions play the dominant role

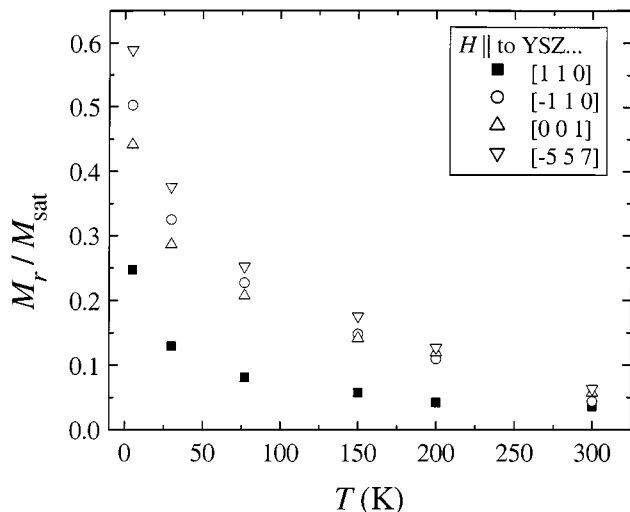


Fig. 5. Remanent magnetization as a function of temperature.  $M_r$  along the surface and along the normal are very different, but there is a secondary effect of orientation within the surface.

despite the relatively low volume fraction in our sample, is in accordance with the conclusions drawn from micromagnetic calculations [10] of the quasistatic magnetization curves at zero temperature for an assembly of interacting dipoles.

#### V. SUMMARY

We have investigated the magnetic response of a textured ensemble of single crystal nanoparticles of iron embedded in single crystal YSZ. The magnetization  $M(\mathbf{H}, T)$  of this relatively dilute ( $\approx 10\%$ ) array appears to be dominated by magnetostatic interactions, with a significantly smaller influence from single particle anisotropy.

#### REFERENCES

- [1] B. D. Cullity, *Introduction to Magnetic Materials*: Addison-Wesley Publishing Company, 1972.
- [2] E. P. Wohlfarth, Ed., "Iron, cobalt and nickel," in *Ferromagnetic Materials*: North-Holland Publishing Company, 1980, vol. 1, pp. 1–70.
- [3] D. L. Leslie-Pelecky and R. D. Rieke, "Magnetic properties of nanostructured materials," *Chem. Mater.*, vol. 8, no. 8, pp. 1770–1783, 1996.
- [4] C. Chen, O. Kitakami, and Y. Shimada, "Particle size effects and surface anisotropy in Fe-based granular films," *J. Appl. Phys.*, vol. 84, pp. 2184–2188, Aug. 1998.
- [5] C. L. Chien, "Granular magnetic solids," *J. Appl. Phys.*, vol. 69, pp. 5267–5272, Apr. 1991.
- [6] J. F. Ziegler, "Transport and range of ions in matter, version 96.01," IBM-Research, Yorktown, NY, 1996.
- [7] S. Honda, F. A. Modine, A. Meldrum, J. D. Budai, T. E. Haynes, L. A. Boatner, and L. A. Gea, "Ion-implantation/annealing-induced precipitation of nanophase ferromagnetic particles in yttrium-stabilized  $\text{ZrO}_2$ ," *Mat. Res. Soc. Symp. Proc.*, vol. 540, pp. 225–230, 1999.
- [8] S. Honda, F. A. Modine, A. Meldrum, J. D. Budai, T. E. Haynes, and L. A. Boatner, "Magneto-optical effects from nanophase  $\alpha$ -Fe and  $\text{Fe}_3\text{O}_4$  precipitates formed in yttrium-stabilized  $\text{ZrO}_2$  by ion implantation and annealing," *Appl. Phys. Lett.*, vol. 77, pp. 711–713, July 2000.
- [9] M. P. Sharrock, "Particle-size effects on the switching behavior of uniaxial and multiaxial magnetic recording materials," *IEEE Trans. Magn.*, vol. 20, no. 5, pp. 754–756, Sept. 1984.
- [10] T. C. Schulthess, M. Benakli, P. B. Visscher, K. D. Sorge, J. R. Thompson, F. A. Modine, T. E. Haynes, L. A. Boatner, G. M. Stocks, and W. H. Butler, "On the role of magnetostatic interactions in assemblies of iron nanoparticles," *J. Appl. Phys.*, to be published.